much structural changes (nonmyocytes size, density, and coupling) are needed to significantly affect the CV. This remarkable simplicity, however, does not extend to repolarization, which was previously found to depend on both the myocyte and the nonmyocyte membrane kinetics [7], [8], [10].

The configuration studied in this paper is relevant to cell culture models covered by a layer of nonmyocytes. Another clinically relevant configuration involves the intermingling of myocytes and nonmyocytes. Propagation across a myocyte–fibroblast–myocyte bridge, however, may require very large myocyte–nonmyocyte coupling. In a computer model, Sachse *et al.* found that propagation across a bridge did not occur in the low coupling regime ($G_c < 2$ nS) where the passive load model is valid, but did occur when the coupling was at least 20 nS.

REFERENCES

[1] P. Kohl, P. Camelliti, F. L. Burton, and G. L. Smith, "Electrical coupling of fibroblasts and myocytes: Relevance for cardiac propagation," *J. Electrocardiol.*, vol. 38, pp. 45–50, 2005.

[2] M. B. Rook, A. C. van Ginneken, B. de Jonge, A. el Aoumari, D. Gros, and H. J. Jongsma, "Differences in gap junction channels between cardiac myocytes, fibroblasts, and heterologous pairs," *Amer. J. Physiol.*, vol. 263, no. 5, pp. C959–C977, 1992.

[3] M. Miragoli, G. Gaudesius, and S. Rohr, "Electrotonic modulation of cardiac impulse conduction by myofibroblasts," *Circ. Res.*, vol. 98, no. 6, pp. 801–810, 2006.

[4] E. Kizana, S. L. Ginn, D. G. Allen, D. L. Ross, and I. E. Alexander, "Fibroblasts can be genetically modified to produce excitable cells capable of electrical coupling," *Circulation*, vol. 111, no. 4, pp. 394–398, 2005.

[5] A. Rosenzweig, "Cardiac cell therapy-mixed results from mixed cells," *N. Engl. J. Med.*, vol. 355, no. 12, pp. 1274–1277, 2006.

[6] W. R. Mills, N. Mal, M. J. Kiedrowski, R. Unger, F. Forudi, Z. B. Popovic, M. S. Penn, and K. R. Laurita, "Stem cell therapy enhances electrical viability in myocardial infarction," *J. Mol. Cell. Cardiol.*, vol. 42, no. 2, pp. 304–314, 2007.

[7] K. A. MacCannell, H. Bazzazi, L. Chilton, Y. Shibukawa, R. B. Clark, and W. R. Giles, "A mathematical model of electrotonic interactions between ventricular myocytes and fibroblasts," *Biophys. J.*, vol. 92, no. 11, pp. 4121–4132, 2007.

[8] F. B. Sachse, A. P. Moreno, and J. A. Abildskov, "Electrophysiological modeling of fibroblasts and their interaction with myocytes," *Ann. Biomed. Eng.*, vol. 36, no. 1, pp. 41–56, 2008.

[9] P. Kohl, A. G. Kamkin, I. S. Kiseleva, and D. Noble, "Mechanosensitive fibroblasts in the sino-atrial node region of rat heart: Interaction with cardiomyocytes and possible role," *Exp. Physiol.*, vol. 79, no. 6, pp. 943–956, 1994.

[10] V. Jacquemet and C. S. Henriquez, "Modelling cardiac fibroblasts: Interactions with myocytes and their impact on impulse propagation," *Europace*, vol. 9, no. 6, pp. vi29–vi37, 2007.

[11] V. Jacquemet and C. S. Henriquez, "Loading effect of fibroblast–myocyte coupling on resting potential, impulse propagation and repolarization: Insights from a microstructure model," *Amer. J. Physiol. Heart Circ. Physiol.*, vol. 294, no. 5, pp. H2040–H2052, 2008.

[12] V. Jacquemet and C. S. Henriquez, "An efficient technique for determining the steady-state membrane potential profile in tissues with multiple cell types," *Comput. Cardiol.*, vol. 34, pp. 113–116, 2007.

[13] Y. Shibukawa, E. L. Chilton, K. A. MacCannell, R. B. Clark, and W. R. Giles, "K^+ currents activated by depolarization in cardiac fibroblasts," *Biophys. J.*, vol. 88, no. 6, pp. 3924–3235, 2005.

[14] S. V. Pandit, R. B. Clark, W. R. Giles, and S. S. Demir, "A mathematical model of action potential heterogeneity in adult rat left ventricular myocytes," *Biophys. J.*, vol. 81, no. 6, pp. 3029–3051, 2001.

[15] V. Jacquemet, "Steady-state solutions in mathematical models of atrial cell electrophysiology and their stability," *Math. Biosci.*, vol. 208, no. 1, pp. 241–269, 2007.

[16] R. J. Ramirez, S. Nattel, and M. Courtemanche, "Mathematical analysis of canine atrial action potentials: Rate, regional factors, and electrical remodeling," *Amer. J. Physiol. Heart Circ. Physiol.*, vol. 279, no. 4, pp. H1767–H1785, 2000.

On ECG Signal Compression With 1-D Multiscale Recurrent Patterns Allied to Preprocessing Techniques

Eddie B. L. Filho, Nuno M. M. Rodrigues, *Member, IEEE*, Eduardo A. B. da Silva*, *Member, IEEE*, Murilo B. de Carvalho, Sérgio M. M. de Faria, *Member, IEEE*, and Vitor M. M. da Silva

***Abstract*—This paper presents the results of a multiscale pattern-matching-based ECG encoder, which employs simple preprocessing techniques for adapting the input signal. Experiments carried out with records from the Massachusetts Institute of Technology-Beth Israel Hospital database show that the proposed scheme is effective, outperforming some state-of-the-art schemes described in the literature.**

***Index Terms*—Data compression, ECG, preprocessing, recurrent patterns.**

I. INTRODUCTION

The ECG is a very important tool for diagnosing heart deceases like ischemia, arrhythmias, and carditis, as well as for monitoring drug effects or pacemaker activity. It is a graphical representation of the electrical stimuli sent by a group of cells referred to as the sinus node, located on the upper portion of the right atrium, which coordinates the heartbeat.

The ECG is a well-structured signal that can be decomposed into five different component waves, named **P**, **Q**, **R**, **S**, and **T** waves. Because of this, many authors have suggested preprocessing techniques to reshape (e.g., as a 2-D array) the original signal in order to exploit its redundancies [1]–[4]. This kind of preprocessing is also often associated with the use of state-of-the-art image encoders, like JPEG2000 [1]–[3] and H.264 intraframe encoder [3], because inter- and intrabeat dependencies may be more efficiently exploited with 2-D assemblies. The adaptation step allows the chosen encoder to better use its compression tools, generating a more compact representation for a given quality.

In this paper, we have used a compression algorithm called multidimensional multiscale parser (MMP) [5], [6], which is based on *multiscale recurrent pattern matching*. It is preceded by an adaptation step, which reshapes the original signal and reveals its inherent structure. We then incorporate one recently developed [3] and one new preprocessing technique to this base framework: the dc equalization and the similarity sorting.

This paper is organized as follows. In Section II, the basic MMP-based framework for compressing ECG signals is presented. In Section III, the used preprocessing techniques, named dc equalization and similarity sorting, are introduced. Section IV describes simple steps on how decoding can be performed. In Section V, we present

Manuscript received April 3, 2008; revised July 22, 2008. Current version published April 15, 2009. *Asterisk indicates corresponding author.*

E. B. L. Filho is with the Centro de Ciência, Tecnologia e Inovação do Pólo Industrial de Manaus, 69057-040 Manaus-AM, Brazil (e-mail: eddie@ctpim.org.br).

N. M. M. Rodrigues and S. M. M. de Faria are with the Instituto de Telecomunicações and Escola Superior de Tecnologia e Gestão de Leiria, Instituto Politécnico Leiria, 2411-901 Leiria, Portugal (e-mail: nuno.rodrigues@co.it.pt; sergio.faria@co.it.pt).

*E. A. B. da Silva is with the Universidade Federal do Rio de Janeiro, 21941-972 Rio Grande do Sul, Brazil (e-mail: eduardo@lps.ufrj.br).

M. B. de Carvalho is with the Universidade Federal Fluminense, 24210-240 Niteroi, Brazil (e-mail: murilo@telecom.uff.br).

V. M. M. da Silva is with the Instituto de Telecomunicações and Department of Engineering Electrotécnica e de Computadores, Universidade de Coimbra, 3030-290 Coimbra, Portugal (e-mail: vitor.silva@co.it.pt).

Digital Object Identifier 10.1109/TBME.2008.2005939

experimental results and comparisons to state-of-the-art encoders. Finally, in Section VI, we present our conclusions.

II. Basic Framework

The basic framework for ECG compression is composed by a preprocessing step and the base MMP algorithm. The former performs the adaptation of the signal and the latter carries through the encoding.

A. Adaptation Step

As was previously mentioned, the ECG signal can be decomposed into sets of compound subwaves, which occur for every heartbeat along the exam, resulting in a quasi-periodic behavior. However, if some pathology is present, the signal may vary considerably. This usually decreases the performance of ECG encoders, because the signal becomes harder to compress.

Length-normalization procedures deal with this problem and help to highlight the structure of the ECG signal. First, all periods are detected, with the algorithms in [7], and then they are normalized to the same length, using the method described in [6]. The original ECG segment $X = [x(0)\ x(1)\ \cdots\ x(N_o-1)]$ is converted into a normalized segment $X_n = [x_n(0)\ x_n(1)\ \cdots\ x_n(N_n-1)]$ using

$$\begin{aligned} X_n(m) &= \hat{X}(h^*) \\ h^* &= \frac{m(N_o-1)}{(N_n-1)} \end{aligned} \tag{1}$$

where $\hat{X}(h^*)$ is the interpolated version of $X(n)$, N_o is the original period length, N_n is the normalized period length, and $m = 0, 1, \ldots, N_n - 1$. The interpolation is computed using cubic-splines and N_n is chosen as the integer part of the average of all period lengths.

After that, the dynamic range of the ECG is reduced. This is important for MMP because the new dictionary elements get more clustered around the average value of the residues and MMP quickly adapts to these patterns. It is done by computing the *average normalized period segment*

$$X_{n_{\text{avg}}}(m) = \frac{1}{M}\sum_{k=0}^{M-1} X_n^k(m) \tag{2}$$

where M is the number of detected periods, X_n^k is the kth normalized period, and $m = 0, 1, \ldots, N_n - 1$. Each *normalized reduced-dynamic-range segment* is computed as the *normalized period segment* subtracted by the *average normalized period segment*

$$X_{n_{rdr}}^k(m) = X_n^k(m) - X_{n_{\text{avg}}}(m) \tag{3}$$

where $m = 0, 1, \ldots, N_n - 1$.

B. MMP Encoder

The MMP algorithm [5], [6] is a universal lossy compression method built upon the *multiscale recurrent pattern matching* concept, in which two vectors with different lengths can be matched. This is possible through the use of a *scale transformation* $T^N(\mathbf{x}) : \mathbb{R}^{\ell(\mathbf{x})} \mapsto \mathbb{R}^N$ [5].

The MMP algorithm associates a binary segmentation tree $\mathcal{S}$ to each input vector $\mathbf{X}^0$. Each node n_j of $\mathcal{S}$ corresponds to a segment $\mathbf{X}^j$ of the input vector. Therefore, MMP must encode the segmentation tree as well as the variable-length vectors corresponding to each leaf node. The segmentation tree is encoded by a sequence of binary flags in a top-down fashion. For the encoding of each segment, MMP uses a set $\mathcal{D} = \{\mathcal{D}^k, k = 0, 1, \ldots, \log_2(N)\}$ of dictionaries $\mathcal{D}^k = \{\mathbf{v}_0^k, \mathbf{v}_1^k, \ldots, \mathbf{v}_{m-1}^k\}$ with m vectors $\mathbf{v}_i$ at scale k. When attempting to encode the segment $\mathbf{X}^j$, MMP searches in the dictionary $\mathcal{D}_R^{s_j}$, which is built from $\mathcal{D}^{s_j}$, for the best vector $\mathbf{v}_{i_j}^{s_j}$ to replace $\mathbf{X}^j$.

The best segmentation tree is found with the minimization of the *Lagrangian* cost $J(n_j)$ defined as

$$D(n_j) = d\left(\mathbf{X}^j, \mathbf{v}_{i_j}^{s_j}\right) \tag{4}$$

$$R(n_j) = -\log_2\left(\Pr\left\{\mathbf{v}_{i_j}^{s_j}\right\}\right) \tag{5}$$

$$J(n_j) = D(n_j) + \lambda R(n_j) \tag{6}$$

where $\mathbf{v}_{i_j}^{s_j}$ is the vector $\mathbf{v}_{i_j}$ at scale j, $d(\mathbf{u}, \mathbf{v})$ is the squared error, and $\Pr\left\{\mathbf{v}_{i_j}^{s_j}\right\}$ is the probability of the vector of index i_j, at scale s_j, being chosen for encoding a given signal segment. The Lagrangian cost of the segmentation tree $\mathcal{S}$ is defined as $J(\mathcal{S}) = D(\mathcal{S}) + \lambda R(\mathcal{S})$, where $D(\mathcal{S})$ is the distortion obtained when using $\mathcal{S}$, $R(\mathcal{S})$ is the rate (flags and indexes), and λ is the Lagrangian multiplier, which controls the tradeoff between distortion and rate. High λ's result in high compression with high distortion, and small values result in low compression with low distortion.

The segmentation tree $\mathcal{S}$ is optimized in a rate-distortion sense by pruning the children nodes n_{2j+1} and n_{2j+2} whenever their Lagrangian cost is greater than that of the parent node n_j [5]. An analysis is also carried out to verify if any two neighbor nodes that do not share the same parent node can be joined together (encoded as only one dictionary index) [8], lowering the global Lagrangian cost.

The dictionary $\mathcal{D}_R^{s_k}$ is built by choosing the N_R vectors $\mathbf{v}_i^{s_k} \in \mathcal{D}^{s_k}$ that best match the causal neighborhood of the element X_k being encoded, in the same way as done in [5].

The encoding process starts with a very simple initial dictionary $\mathcal{D}$ composed by the 1×1 elements with amplitudes $\{0, 4, 8, \ldots, 2^M - 1\}$; when expanded to the other scales, they generate dictionaries having only constant elements. The dictionaries are updated with the concatenation of the reconstructed segments $\hat{\mathbf{X}}^{2j+1}$ and $\hat{\mathbf{X}}^{2j+2}$, associated to the children nodes n_{2j+1} and n_{2j+2}, giving rise to $\hat{\mathbf{X}}^j$ as the reconstructed segment associated to the parent node n_j. It is then included in every dictionary $\mathcal{D}^{s_k}$ through the scale transformation [5].

One may thus associate an origin scale to any element in the dictionary from which it is transformed. Then, it is possible to access it using two components: *origin scale* and *index*. This way, the rate needed to specify the element becomes

$$R(n_j) = -\left(\log_2(\Pr(\mathcal{D}^{s_j,s_l})) + \log_2\left(\Pr\left(\mathbf{v}_{i_j}^{s_j,s_l}\right)\right)\right) \tag{7}$$

where $\Pr(\mathcal{D}^{s_j,s_l})$ is the probability that the element chosen for encoding $\mathbf{X}^j$, at scale s_j, belongs to the dictionary partition with elements transformed from scale s_l and $\Pr(\mathbf{v}_{i_j}^{s_j,s_l})$ is the probability of element $\mathbf{v}_{i_j}^{s_j,s_l}$ of the dictionary partition at scale s_j, with elements transformed from scale s_l being chosen for encoding a given signal block. So, the use of an adaptive arithmetic encoder for each component has the potential to reduce the rate needed to specify dictionary elements.

A *displacement dictionary* $\mathcal{D}_D$ [5], for improving the exploitation of the interbeat redundancies, is also used when encoding a segment $\mathbf{X}^j$. It contains displaced versions of the approximations for previously encoded segments and is implemented by keeping the M last samples of the reconstructed signal. This auxiliary dictionary also participates in the creation of $\mathcal{D}_R^{s_k}$.

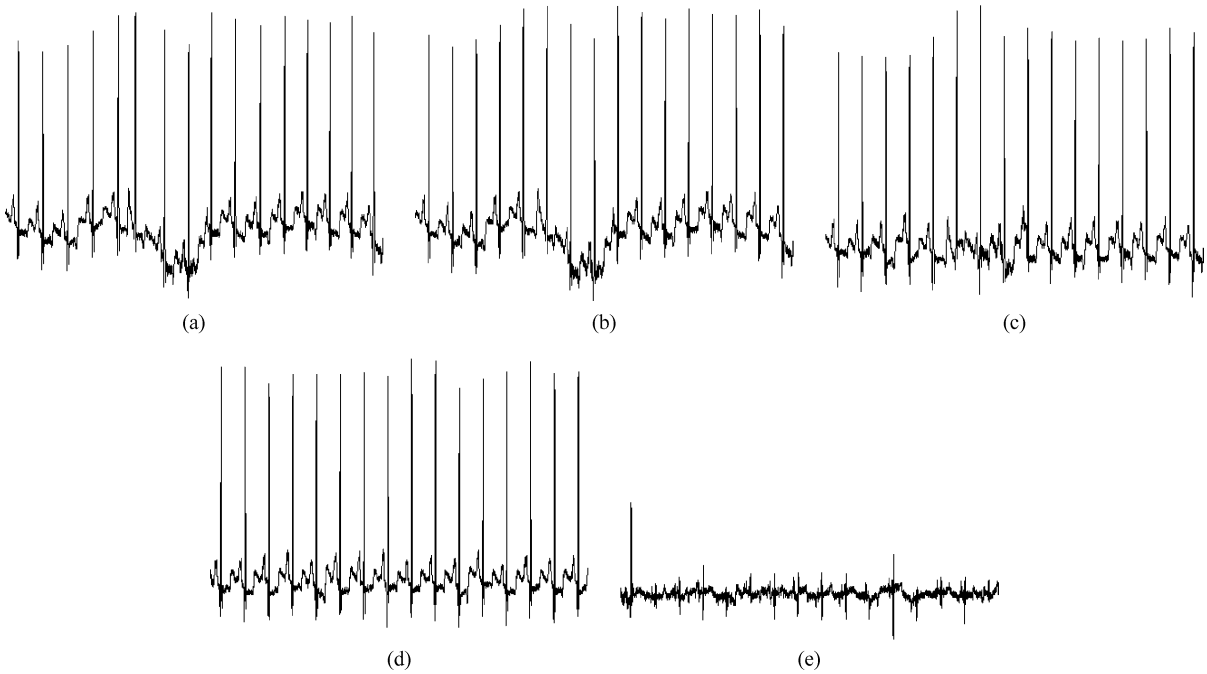

Fig. 1. Effect of preprocessing techniques on record 100 from the Massachusetts Institute of Technology-Beth Israel Hospital database. (a) Original signal. (b) Length-normalized signal. (c) DC-equalized signal. (d) Similarity-ordered signal. (e) Reduced-dynamic-range signal.

III. Further Adaptations: DC Equalization and Similarity Sorting

Fig. 1(a) and (b) shows an original ECG signal and the result of the length-normalization procedure, respectively. One can realize that the normalized signal still presents a great deal of variation, which is mainly noticeable on the dc level of heartbeat periods. This behavior is normal as the condition of the patient varies along the exam; however, it can impair the performance of the encoder because the apparent correlation among periods decreases.

If the dc levels are the same, the probability that elements used to approximate segments of a period are used on the next ones increases, favoring the coding/prediction scheme used by MMP. This correction can be done through the use of a dc equalization procedure (as done in [3]). The original dc levels of the detected ECG periods are calculated according to

$$\mathrm{dc}_k = \left\lfloor \frac{1}{L_N} \sum_{i=1}^{L_N} x_k(i) \right\rfloor \tag{8}$$

where $x_k(i)$ are the signal samples of period k and L_N is the normalized length. Then, all periods are clamped to the minimum possible dc level by

$$x_k^{\mathrm{dc}}(i) = x_k(i) - (\mathrm{dc}_k - \mathrm{dc}_{\min}) + \delta \tag{9}$$

where $x_k^{\mathrm{dc}}(i)$ are the dc-equalized period samples, $\mathrm{dc}_{\min}$ is the minimum dc level, and δ is a constant to guarantee that the minimum value is greater than or equal to zero. The result of this preprocessing technique is shown in Fig. 1(c).

Although the dc equalization corrects the level of all periods, adjacent lines may still be very different. It happens because the condition of the patient changes from one heartbeat to the other and the length normalization is not able to correct the shape of the signal. One can notice that by evaluating Fig. 1(c), where periods located at the center present a different shape when comparing to the others. This still reduces the correlation among heartbeats, and consequently, the efficiency of MMP. This problem can be addressed by rearranging periods based on a metric that reflects their similarity. After the dc equalization, the variances of the periods are computed and the segment with the smallest one is positioned as the first heartbeat. The following periods are then positioned in descending order of similarity with the previous one; it has been verified that a good similarity metric for the mth period in this case is the mse given by

$$\mathrm{MSE}_k = \frac{1}{L_N} \sum_{i=1}^{L_N} \left(x_k(i) - x_{m-1}(i)\right)^2 \tag{10}$$

where $x_{m-1}(i)$ are the samples of the $(m-1)$th reordered period and $x_k(i)$ are the samples of the kth ECG period. We refer to this step as similarity sorting, because periods are reordered according to a similarity metric related to the previous one. Its effect on the dc-equalized signal of Fig. 1(c) is illustrated in Fig. 1(d). It can be observed that now adjacent periods are more similar, and patterns learned by MMP on any period may be easily used for encoding subsequent ones. Besides, the shape of periods varies smoothly along the signal (its variance increases as encoding proceeds), allowing MMP to quickly adapt to the current behavior. Fig. 1(e) shows the reduced-dynamic-range signal [see (3)].

It is worth noting that this sorting procedure is slightly different from the one in [3]. There, periods are reordered with respect to their variances (complexity sorting); however, the procedure presented in this paper relies on their similarity, it being more suitable to 1-D schemes. One can also argue that the *average normalized period segment* presented in Section II-A is capable of reducing the dynamic range of the signal only if it is quasi-periodic. Indeed, if the signal varies a great deal, the dynamic range reduction is impaired. However, the period normalization in conjunction with the dc equalization tend to greatly improve the correlation among periods, which still provides good results when dealing with irregular signals.

TABLE I
PERFORMANCE COMPARISON OF DIFFERENT ECG COMPRESSION SCHEMES

Algorithm	Record	CR	PRD
Chou et. al app. 2 [1]	100	24 : 1	4.06
T3 - JPEG2000 [3]	100	24 : 1	3.95
T1 - H.264 [3]	100	24 : 1	3.47
MMP [6]	100	24 : 1	3.40
DCeq - MMP	100	24 : 1	3.30
T3 - JPEG2000 [3]	100	10 : 1	2.12
T1 - H.264 [3]	100	10 : 1	2.08
MMP [6]	100	10 : 1	2.10
DCeq - MMP	100	10 : 1	2.03
MMP [6]	102	22.49 : 1	3.02
DCeq/SS - MMP	102	22.49 : 1	2.49
Tai et. al [9]	107	10.7 : 1	1.90
MMP [6]	107	10.7 : 1	1.70
DCeq - MMP	107	10.7 : 1	1.61
Tai et. al [9]	115	30.6 : 1	4.10
MMP [6]	115	30.6 : 1	3.20
DCeq/SS - MMP	115	30.6 : 1	2.92
T3 - JPEG2000 [3]	117	24 : 1	1.72
T1 - H.264 [3]	117	24 : 1	1.64
MMP [6]	117	24 : 1	1.42
DCeq - MMP	117	24 : 1	1.26
Chou et. al app. 2 [1]	117	13 : 1	1.18
T3 - JPEG2000 [3]	117	13 : 1	1.07
T1 - H.264 [3]	117	13 : 1	1.14
MMP [6]	117	13 : 1	0.99
DCeq - MMP	117	13 : 1	0.91
Wei et. al [4]	117	10 : 1	1.18
Bilgin et. al [2]	117	10 : 1	1.03
Chou et. al app. 1 [1]	117	10 : 1	0.98
T3 - JPEG2000 [3]	117	10 : 1	0.86
T1 - H.264 [3]	117	10 : 1	0.95
MMP [6]	117	10 : 1	0.86
DCeq - MMP	117	10 : 1	0.79
Bilgin et. al [2]	117	8 : 1	0.86
T3 - JPEG2000 [3]	117	8 : 1	0.75
T1 - H.264 [3]	117	8 : 1	0.81
MMP [6]	117	8 : 1	0.76
DCeq - MMP	117	8 : 1	0.72
Lee et. al [10]	119	24 : 1	10.5
Bilgin et. al [2]	119	21.6 : 1	3.76
Tai et. al [9]	119	20 : 1	2.17
Chou et. al app. 2 [1]	119	20.9 : 1	1.81
T3 - JPEG2000 [3]	119	20.9 : 1	1.92
T3 - H.264 [3]	119	20.9 : 1	1.78
MMP [6]	119	20.9 : 1	2.43
DCeq/SS - MMP	119	20.9 : 1	1.83
Chou et. al app. 2 [1]	119	10 : 1	1.03
Norm. - JPEG2000	119	10 : 1	1.37
T3 - JPEG2000 [3]	119	10 : 1	0.93
T3 - H.264 [3]	119	10 : 1	1.00
MMP [6]	119	10 : 1	1.27
DCeq/SS - MMP	119	10 : 1	1.07
T3 - JPEG2000 [3]	119	8 : 1	0.74
T3 - H.264 [3]	119	8 : 1	0.83
MMP [6]	119	8 : 1	1.08
DCeq/SS - MMP	119	8 : 1	0.91

IV. DECODING PROCESS

The decoding of the compressed signal is performed by first processing the MMP bit stream, which complies recovery of the segmentation tree $\mathcal{S}$, using the binary flags, and assignment of a dictionary element for each index i_j. While decoding is performed, concatenations of the assigned blocks are added to the dictionary, in the same way as done during encoding. The decompressed signal is then resorted (if needed), the dc equalization is removed, and the original period lengths are recovered, in this very order, using the information added to the header of the compressed file, which finally results in the reconstructed signal.

V. EXPERIMENTAL RESULTS

The efficiency of the proposed framework was assessed by running tests with the first 216 000 samples (10 min) from records 100, 102, 107, 115, 117, and 119 of the Massachusetts Institute of Technology-Beth Israel Hospital (MIT-BIH) ECG database. They were chosen because there are compression results reported for them in the literature [1]–[4], [9], [10]. The signals were sampled at 360 Hz with 11 bits of resolution. The original length of each period, the original dc levels and the clamp level are differentially and arithmetically encoded and sent as side information to the decoder. The original ordering is encoded with an adaptive-model arithmetic encoder, which accounts for the previous occurrence of an index by setting its probability to zero once it is used. Each input signal is then split into segments of 64 samples, which are sequentially processed by the algorithm. The quality of the reconstructed signals is evaluated by using the percent rms difference (PRD), commonly adopted in the literature, defined as

$$\mathrm{PRD} = \sqrt{\frac{\sum_{i=0}^{N-1}\left(x(i)-\hat{x}(i)\right)^2}{\sum_{i=0}^{N-1}\left(x(i)-\mu\right)^2}} \times 100\% \tag{11}$$

where $x(n)$ and $\hat{x}(n)$ are the original and the reconstructed signals, respectively, N is their length, and μ is the baseline value of the analog-to-digital conversion used for the acquisition of the data $x(n)$ ($\mu = 1024$ for the chosen records). Although the signal is segmented for being processed by MMP, the PRD is indeed calculated over the complete sequence, i.e., 10 min (and not in a block-by-block basis). The compression ratio (CR) is evaluated as

$$\mathrm{CR} = \frac{B_o}{B_c} \tag{12}$$

where B_o is the total number of bits in the original signal and B_c is the total number of bits in the compressed format, including side information. For each of the test signals, $B_o = 11 \times 216\,000$, corresponding to 11 bits resolution and the first 10 min. The results are summarized in Table I. The proposed algorithm outperformed all other tested methods for records 100, 102, 107, 115, and 117, and got comparable results when compressing record 119. The comparisons with [9] took into account the block size suggested by that author (32×256). Although the tested methods tend to have close results at low compression ratios, the proposed method is superior at high compression ratios, while keeping a reasonable PRD (do not compromise the diagnosis), which is the main goal in ECG compression. One can see from Table I that the similarity sorting (SS) is not always used. Tests showed that this technique is advantageous only when the standard deviation of period lengths is greater than 8%, so it should be skipped when this was not the case. Due to its overhead, it can cause a decrease in the PRD of approximately 0.05%–0.1%. It is worth noting that the algorithm in [9] employs a more advanced method for the QRS detection and the compression performance varies with the block size.

One should note that the computational complexity associated to the proposed techniques is low. The dc equalization is composed by one division per period and summations [see (8) and (9)]. The complexity

of the sorting procedure is higher and is heavily influenced by the operations described by (10), which are peformed for the m remaning periods, at each step. However, these computations can be greatly speed up with the use of lookup tables, keeping the global complexity low; decoding is simpler and consists of just assigning the original position and level of each segment.

VI. Conclusion

We incorporated new preprocessing techniques to an existing ECG compression framework, which led to an enhancement on the quality of the reconstructed signals. The proposed techniques are simple and present a small increase in computational complexity. The results obtained were encouraging, showing that the final framework, when compared to the state of the art, gives quite competitive results. Besides, this paper reveals that it is worthy pursuing new preprocessing techniques for ECG compression, which can cluster/reshape similar heartbeat periods and reveal structures that are not apparent in the raw ECG signal.

References

[1] H.-H. Chou, Y.-J. Chen, Y.-C. Shiau, and T.-S. Kuo, "An effective and efficient compression algorithm for ECG signals with irregular periods," *IEEE Trans. Biomed. Eng.*, vol. 53, no. 6, pp. 1198–1205, Jun. 2006.

[2] A. Bilgin, M. W. Marcellin, and M. I. Altbach, "Compression of electrocardiogram signals using JPEG2000," *IEEE Trans. Consum. Electron.*, vol. 49, no. 4, pp. 833–840, Nov. 2003.

[3] E. B. L. Filho, N. M. M. Rodrigues, E. A. B. da Silva, S. M. M. de Faria, V. M. M. da Silva, and M. B. de Carvalho, "ECG signal compression based on dc equalization and complexity sorting," *IEEE Trans. Biomed. Eng.*, vol. 55, no. 7, pp. 1923–1926, Jul. 2008.

[4] J.-J. Wei, C.-J. Chang, N.-K. Chou, and G.-J. Jan, "ECG data compression using truncated singular value decomposition," *IEEE Trans. Inf. Technol. Biomed.*, vol. 5, no. 4, pp. 290–299, Dec. 2001.

[5] E. B. L. Filho, E. A. B. da Silva, M. B. Carvalho, W. S. S. Júnior, and J. Koiller, "Electrocardiographic signal compression using multiscale recurrent patterns," *IEEE Trans. Circuits Syst. I, Reg. Papers*, vol. 52, no. 12, pp. 2739–2753, Dec. 2005.

[6] E. B. L. Filho, E. A. B. da Silva, W. S. S. Júnior, and M. B. de Carvalho, "ECG compression using multiscale recurrent patterns with period normalization," in *Proc. IEEE Int. Symp. Circuits Syst.*, Kos, Greece, May 2006, pp. 1607–1610.

[7] M. Aboy, C. Crespo, J. McNames, J. Bassale, L. Jenkins, and B. Goldsteins, "A biomedical signal processing toolbox," in *Proc. Biosignal 2002*, Jun., pp. 49–52.

[8] R. Shukla, P. L. Dragotti, M. N. Do, and M. Vetterli, "Rate-distortion optimized tree-structured compression algorithms for piecewise polynomial images," *IEEE Trans. Image Process.*, vol. 14, no. 3, pp. 343–359, Mar. 2005.

[9] S.-C. Tai, C.-C. Sun, and W.-C. Tan, "2-D ECG compression method based on wavelet transform and modified SPIHT," *IEEE Trans. Biomed. Eng.*, vol. 52, no. 6, pp. 999–1008, Jun. 2005.

[10] H. Lee and K. M. Buckley, "ECG data compression using cut and align beats approach and 2-D transforms," *IEEE Trans. Biomed. Eng.*, vol. 46, no. 5, pp. 556–565, May 1999.

Improved Event Interval Reconstruction in Synthetic Electrocardiograms

Michael Potter, *Student Member, IEEE*,
and Witold Kinsner*, *Senior Member, IEEE*

***Abstract*—Mathematical models for synthesizing ECGs are important tools in providing reproducible standard signals for biomedical signal processing research and technology. The ECG synthesis model ECGsyn and its extensions are the state of the art and realistically capture: 1) the ECG morphology; 2) the spectrum of heart rate variability; and 3) QT-interval adaptation to heart rate. This paper demonstrates ECGsyn's time-domain limitations at reconstructing an ECG time series from ECG wave annotations. An alternative algorithm, ECGfm, is therefore presented that recreates the event intervals with greater fidelity by applying the wave annotations as a phase constraint. Results on data drawn from the Physionet Physobank QT database demonstrate the improved performance of the ECGfm algorithm.**

***Index Terms*—Electrocardiogram ECG modeling, event intervals (EIs), heart-rate variability (HRV), RR-intervals.**

I. Introduction

The analysis of cardiac health is based primarily on the regular morphology of the *electrocardiogram* (ECG) [1]. Secondary information on cardiac regulation is also analyzed in the form of *heart rate variability* (HRV) [2]. A recent model for the synthesis of ECG that successfully captures both the regular morphology of the ECG waves as well as the spectral properties of HRV in ECGsyn [3]. This model has been extended into: 1) a 3-D cardiac dipole vector model [4]; and 2) a system that accepts an RR-interval sequence input so that the synthesized ECG can fit recorded intervals [5], [6]. The second approach is of interest because it provides a systematic method for the transcription of beat annotations back into an ECG times series with applications in technology standardization, education, and research [6].

This paper presents a comparison of reconstructed synthetic ECG *event intervals* (EIs) to the original template, and identifies two time-domain limitations of the ECGsyn model [5]. First, the RR-intervals of the synthetic ECG can be systematically different from the original ECG being reconstructed. Second, the synthetic ECG distributes the RR-variability linearly throughout the ECG beat irrespective of the original EI relationship. This paper also presents an alternative algorithm, called ECGfm, that overcomes these limitations by constraining the EI behavior of the synthetic ECG.

II. EIs and Synthetic IHR

Consider an ECG signal with R-wave (QRS-complex) occurrence times t_n, $n \geq 0$. Typically, HRV is represented as a sequence of RR-intervals, $\Delta_R(n) = t_n - t_{n-1}$, $n \geq 1$, extracted from the ECG signal [7]. This sequence of discrete events, the *tachogram*, is well ordered by

Manuscript received February 22, 2008; revised May 21, 2008. First published October 31, 2008; current version published April 15, 2009. This work was supported by the Natural Sciences and Engineering Research Council (NSERC) of Canada. *Asterisk indicates corresponding author*.

M. Potter is with the Department of Electrical and Computer Engineering, University of Manitoba, Winnipeg, MB R3T 5V6, Canada (e-mail: m.potter@ieee.org).

*W. Kinsner is with the Department of Electrical and Computer Engineering, University of Manitoba, Winnipeg, MB R3T 5V6, Canada (e-mail: kinsner@ee.umanitoba.ca).

Color versions of one or more of the figures in this paper are available online at http://ieeexplore.ieee.org.

Digital Object Identifier 10.1109/TBME.2009.2003088